ELSEVIER

Biochemical Pharmacology 61 (2001) 299–310

Biochemical Pharmacology

Apoptotic response of HL-60 human leukemia cells to the antitumor drug NB-506, a glycosylated indolocarbazole inhibitor of topoisomerase 1

Michael Facompre[a], Jean-François Goossens[b], Christian Bailly[a,*]

[a]*INSERM U-524, Laboratoire de Pharmacologie Antitumorale du Centre Oscar Lambret, IRCL, Place de Verdun, F-59045 Lille, France*
[b]*Laboratoire de Chimie Analytique, Faculté de Pharmacie, F-59045 Lille, France*

Received 17 March 2000; accepted 5 July 2000

Abstract

The antitumor drug NB-506 is a glycosylated indolocarbazole derivative targeting topoisomerase I. This DNA-intercalating agent, which is currently undergoing phase I/II clinical trials, was shown to induce apoptosis in HL-60 human leukemia cells. We compared the cellular dysfunctions induced by NB-506 and the reference topoisomerase I poison camptothecin (CPT) at the nuclear, mitochondrial, and cytoplasmic levels. The two drugs NB-506 and CPT were almost equally toxic to HL-60 cells and produced similar cell cycle changes with a considerable increase in the fraction of cells with DNA content less than G1. The sub-G1 fraction, which can be considered as the apoptotic cell population, appeared more rapidly with CPT than with NB-506 but in both cases, the cell cycle perturbation was accompanied by a marked decrease in the mitochondrial transmembrane potential and the intracellular pH. In contrast, no change in the intracellular calcium concentration was detected. Treatment of HL-60 cells with NB-506 resulted in an increase in the activity of the intracellular protease caspase-3, as determined by a DEVD-based colorimetric assay and direct monitoring of poly(ADP-ribose) polymerase (PARP) cleavage by Western blot analysis. The initiator caspase-8 was also stimulated by NB-506 but, as for caspase-3, the extent of the caspase activation was weaker with NB-506 compared to CPT. With both drugs, the protease activation resulted in DNA degradation, as independently confirmed via the terminal deoxynucleotidyl transferase-mediated dUTP nick end-labeling (TUNEL) assay and characterization of internucleosomal DNA fragmentation. Collectively, these findings identify some of the molecular events leading to NB-506-induced apoptosis and as such, provide important mechanistic insights into the mode of action of topoisomerase I-targeted indolocarbazole antitumor drugs.

Keywords: Apoptosis; Topoisomerases; Cell cycle; Caspases; DNA fragmentation

1. Introduction

NB-506 (Fig. 1) is a synthetic indolocarbazole that exhibits remarkable activity against experimental cancer xenografts (including colon and lung cancers) and displays a low toxicity profile [1,2]. This compound, which is now undergoing clinical trials for the treatment of human cancers [3,4], is a potent topoisomerase I poison. The anticancer activity of NB-506 and related compounds has been attributed to their capacity to stabilize DNA–topoisomerase I complexes [5,6]. Over the last few years, we have investigated the mode of action of NB-506 and analogues principally at the molecular level [7–9]. The important role of the sugar moiety for inhibition of topoisomerase I and DNA recognition has been fully characterized [10,11]. Recently, we showed that despite their structural differences, indolocarbazoles share common steric and electronic features with the camptothecins, which are by far the best-characterized topoisomerase-targeted antitumor drugs, thus providing a structurally sound model to identify a specific pharmacophore for topoisomerase I inhibitors [12].

* Corresponding author. Tel.: +33 320 16 92 18; fax: +33 320 16 92 29.

E-mail address: bailly@lille.inserm.fr (C. Bailly).

Abbreviations: BCECF, 2′,7′-bis(carboxyethyl)5(6)-carboxyfluorescein; CPT, camptothecin; DEVD-pNA, *N*-acetyl-Asp-Glu-Val-Asp-*para*-nitroaniline; $DiOC_6(3)$, 3,3-dihexyloxacarbocyanine iodide; IETD-pNA, *N*-acetyl-Ile-Glu-Thr-Asp-*para*-nitroaniline; NB-506, 6-*N*-formylamino-12,13-dihydro-1,11-dihydroxy-13-(β-D-glucopyranosyl)-5*H*-indolo[2,3-*a*]pyrrolo-[3,4-*c*]carbazole-5,7-(6*H*)-dione; PARP, poly(ADP-ribose) polymerase; and TUNEL, terminal deoxynucleotidyl transferase-mediated dUTP nick end-labeling.

0006-2952/01/$ – see front matter
PII: S0006-2952(00)00553-0

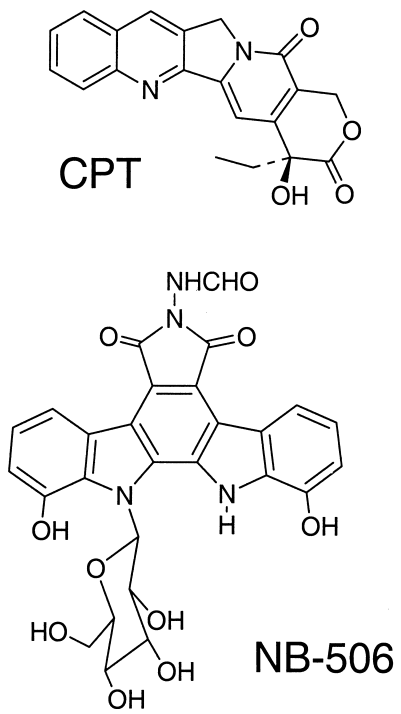

Fig. 1. Structures of camptothecin (CPT) and the antitumor indolocarbazole drug NB-506 [6-*N*-formylamino-12,13-dihydro-1,11-dihydroxy-13-(*β*-D-glucopyranosyl)-5*H*-indolo[2,3-*a*]pyrrolo-[3,4-*c*]carbazole-5,7-(6*H*)-dione].

Two types of NB-506-resistant cell lines have been established. SBC-3/NB#9 cells, selected for their extremely high resistance to NB-506, were found to be cross-resistant to the camptothecin derivatives CPT-11 and 7-ethyl-10-hydroxycamptothecin (SN-38), and the resistance was attributed to markedly reduced topoisomerase I activity and protein content [13]. Very recently, the P388/F11 cell line, also resistant to NB-506, was described. A partial duplication of the topoisomerase I gene was found in these cells, providing a molecular basis to explain the resistance mechanism [14]. The accumulated data strongly suggest that topoisomerase I constitutes the main intracellular target for indolocarbazoles related to NB-506 [15]. However, it is still unclear how the stabilization of topoisomerase I–DNA covalent complexes and the subsequent induction of DNA strand breaks lead to cytotoxicity. It is known that topoisomerase inhibitors can lead to cell death via induction of apoptosis, but the sequence of events involved in the apoptotic process remains to be clarified [16,17].

Here, we continue to dissect the mechanism of action of NB-506 by analyzing the capacity of the drug to induce apoptosis in HL-60 human leukemia cells. The aim of the study was to gain insight into the signaling pathways involved in apoptosis induced by NB-506. The action of the indolocarbazole drug was compared with that of the reference topoisomerase I poison CPT. Specifically, we evaluated the involvement of initiator and effector proteases, caspase-8 and caspase-3, respectively, and we characterized different drug-induced cellular dysfunctions at the nuclear, mitochondrial, and cytoplasmic levels.

2. Materials and methods

2.1. Chemicals

The drug NB-506 was kindly provided by Dr. Tomoko Yoshinari from Banyu Pharmaceuticals (Japan). Its chemical synthesis has been reported [18]. Oligomycin, staurosporine, and camptothecin were purchased from Sigma Chemical Co. CPT and NB-506 were first dissolved in DMSO at 5 mM and then further diluted with water. Stock solutions of the drugs were kept at −20° and diluted with water to the desired concentration immediately prior to use. Nigericin, $DiOC_6(3)$, the acetoxymethyl esters of Fura 2 and BCECF, and carbonyl cyanide *p*-chlorophenylhydrazone (CCCP) were purchased from Molecular Probes. Propidium iodide was from Aldrich. All other chemicals were analytical grade reagents.

2.2. Cell culture and survival assay

Human HL-60 promyelocytic leukemia cells were obtained from the European Collection of Cell Cultures. Cells were grown at 37° in a humidified atmosphere containing 5% CO_2 in RPMI-1640 medium, supplemented with 10% fetal bovine serum, glutamine (2 mM), penicillin (100 UI/mL), and streptomycin (100 μg/mL). The cytotoxicity of the drugs was assessed using a cell proliferation assay developped by Promega (CellTiter 96® AQ_{ueous} one solution cell proliferation assay). Briefly, 2×10^4 exponentially growing cells were seeded in 96-well microculture plates with various drug concentrations in a volume of 100 μL. After 48-hr incubation at 37°, 20 μL of 3-(4,5-dimethylthiazol-2-yl)-5-(3-carboxymethoxyphenyl)-2-(4-sulfophenyl)-2*H*-tetrazolium, inner salt (MTS) [19] was added to each well, and the samples were incubated for a further 2 hr at 37°. Plates were analyzed on a Labsystems Multiskan MS (type 352) reader at 492 nm.

2.3. Cell cycle analysis

For flow cytometry analysis of DNA content, 5×10^5 HL-60 cells in exponential growth were treated with CPT for the indicated period and then washed 3 times with citrate buffer. The cell pellet was incubated with 125 μL of trypsin-containing citrate buffer for 10 min at room temperature and then with 100 μL of citrate buffer containing a trypsin inhibitor and RNase (10 min) prior to adding 100 μL of propidium iodide at 125 μg/mL. Samples were analyzed on a Becton Dickinson FACScan (Fluorescence-Activated Cell Scanner) flow cytometer using the LYSYS II software which is also used to determine the percentage of cells in G1, S, and G2/M phases.

2.4. Mitochondrial membrane potential ($\Delta\Psi mt$) measurements

Mitochondrial energization was determined as the retention of the fluorescent dye $DiOC_6$. After the drug treatment, 10^6 cells in 2 mL of complete RPMI-1640 medium were loaded with the $DiOC_6$ probe (usually 100 nM unless otherwise stated) for 30 min at 37° prior to the flow cytometry analysis. The same incubation time was applied to the controls and the different assays. $DiOC_6$ was excited at 488 nm, and fluorescence was analyzed at 525 nm (F1-1) after logarithmic amplification.

2.5. Intracellular pH measurements

Cells were incubated with the acetomethyl ester derivative of BCECF (BCECF-AM at 2 μM) in 1 mL of culture medium. After 30-min incubation in a CO_2 incubator at 37°, cells were pelleted, rinced once with Hanks' balanced saline solution (HBSS), and resuspended at an appropriate density for fluorescence measurements. Intracellular carboxy-BCECF was excited at 440 and 490 nm simultaneously, whereas the emission was measured at 535 nm with an 8-nm band-pass filter [20]. All spectra were recorded with a SPEX spectrofluorometer. Autofluorescence was measured in unloaded cells and the control value was subtracted from all measurements. Intracellular pH was estimated by comparison of the mean ratio values (fluorescence at 490 nm divided by fluorescence at 440 nm) of a sample to a calibration curve established by incubation of BCECF-AM-loaded cells in varied pH buffer in the presence of the proton ionophore nigericin [21].

2.6. Intracellular calcium measurements

Leukemia cells were incubated for 30 mn at 37° with the cell-permeant fluorescent probe Fura 2-acetomethyl ester (5 μM) mixed with the mild non-ionic surfactant Pluronic F127 (0.02%). The best results for loading were obtained with a Krebs–Ringer buffer containing 132 mM NaCl, 4 mM KCl, 0.5 mM $MgCl_2$, 1 mM $CaCl_2$, 5 mM glucose, and 9.5 mM HEPES (pH 7.4). After a 90-min wash with free dye medium, the fluorescence emitted by loading cells at 37° was measured using a SPEX fluorolog spectrofluorometer. The ratiometric indicator, Fura 2, was excited alternatively at two differents wavelengths (340 and 380 nm, 2-nm slit), and the emission was collected at the fixed wavelength of 550 nm (5-nm slit). Autofluorescence was measured in unloaded cells and this control value was substracted from all measurements. Intracellular Ca^{2+} concentration was calculated using the dissociation equation [22]. Calibration curves were obtained by following the usual procedure [23].

2.7. DEVD-pNA and IETD-pNA cleavage

DEVD-pNA and IETD-pNA cleavage activities were measured using the ApoAlert™ CPP32/caspase-3 and ApoAlert™ Caspase-8 assay kits (Clontech) according to the recommended protocols. Briefly, 2×10^6 exponentially growing HL-60 cells in 2 mL of RPMI-1640 medium were treated with the test drug at the indicated concentration for 4 or 18 hr at 37°. Cells were pelleted by centrifugation and resuspended in 50 μL of the lysis buffer. The lysed cell mixture was then incubated on ice for 10 min prior to centrifugation (11,750 *g*, 3 min at 4°). Fifty microliters of 2X reaction buffer supplemented with 10 mM dithiothreitol was then added to each tube incubated at 4°. During this period, a control was prepared by adding 0.5 μL of 1 mM DEVD-fmk or z-IETD-fmk to a cell sample treated with 0.1 μM staurosporine (24 hr at 37°). The substrate (DEVD-pNA or IETD-pNA) was added to all tubes (5 μL, 50 μM), and the samples were incubated for 1 hr at 37°. The formation of *p*-nitroanilide was measured at 405 nm using a Labsystems Multiskan MS microtiter plate reader.

2.8. PARP cleavage

Briefly, 7×10^5 exponentially growing HL-60 cells (2 mL at 7×10^5 cells/mL) in a serum-free medium were treated with the test drug at the indicated concentration for up to 5 hr at 37°. Cells were pelleted by centrifugation at 4°, resuspended in 3 mL of lysis buffer containing PBS, 0.1 mM phenylmethylsulfonyl fluoride, and the protease inhibitors chymostatin, leupeptin, aprotinin, and pepstatin A (5 μg/mL each). After centrifugation, the pellet was resuspended in the loading buffer containing 50 mM Tris–HCl pH 6.8, 15% sucrose, 2 mM EDTA, 3% SDS, and 0.01% bromophenol blue. The mixture was sonicated for 30 sec at 4° and then boiled to 100° for 3 min. For Western blotting, the cell lysates were fractionated on a 7.5% polyacrylamide gel containing 0.1% SDS, then transferred onto a Hybond-C nitrocellulose membrane (Amersham) for 45 min at 0.8 mA/cm^2 using a semidry transfer system. Membranes were blocked with 10% non-fat milk in PBST (phosphate-buffered saline, pH 7.4 containing 0.1% Tween 20) for 30 min followed by incubation with anti-PARP monoclonal antibody (Clontech) (dilution 1:10,000 in PBST supplemented with 1% non-fat milk) for 30 min. The blots were washed three times (5 min each with PBST) and incubated with a sheep anti-mouse immunoglobulin G conjugated to horseradish peroxidase (Amersham Life Sciences, 1:10,000 dilution in PBST containing 1% non-fat milk) for 30 min. After three successive washes with PBST, the Western blot chemiluminescence reagent from NEN was used for the detection. Bands were vizualized by autoradiography.

2.9. Caspase-8 activation

Exponentially growing HL-60 cells (2×10^6 in 2 mL) in a serum-free medium were treated with the test drug at the indicated concentration for up to 20 hr at 37°. Half of the cells were pelleted by centrifugation at 4° and washed twice with PBS (2×3 mL) at 4°. After centrifugation, the pellet was resuspended in 25 μL of boiling buffer containing 10 mM Tris–HCl pH 7.4, 1 mM Na-vanadate, 1% SDS, 0.1 mM phenylmethylsulfonyl fluoride, and the protease inhibitors leupeptin, aprotinin, and pepstatin A (10 μg/mL each). The mixture was incubated for 10 min at 4° prior to the addition of 80 μL of the electrophoresis dye solution (15% sucrose, 2 mM EDTA, and 0.01% bromophenol blue). Samples were passed through a 26 Gauge needle to reduce the viscosity of the solutions, which were then boiled to 100° for 3 min. For Western blotting, the cell lysates were fractionated on a 12% polyacrylamide gel containing 0.1% SDS, then transferred onto a Hybond-C nitrocellulose membrane (Amersham) for 45 min at 0.8 mA/cm^2 using a semi-dry transfer system. Membranes were blocked with 10% non-fat milk in PBST for 30 min followed by incubation with anti-human caspase-8 monoclonal antibody (Immunotech) (dilution 1:500 in PBST supplemented with 2% non-fat milk) for 4 hr in the dark. The blots were washed three times (15 min each with PBST) and incubated with a sheep anti-mouse immunoglobulin G conjugated to horseradish peroxidase (Amersham Life Sciences, 1:10,000 dilution in PBST containing 2% non-fat milk) for 1 hr. After three successive washes (25 min each) with PBST, the Western blot chemiluminescence reagent from NEN was used for the detection.

2.10. Detection of DNA fragmentation

HL-60 cells at a density of about 10^6 cells/mL were treated with various concentrations of the drug for the indicated periods and then collected by centrifugation at 2500x*g* for 5 min. The resultant cell pellets were resuspended in PBS buffer containing 5 mM $MgCl_2$ and lysed in 500 μL of TE buffer containing 0.1% SDS and proteinase K (1.5 mg/mL) overnight at 37°. After two successive extractions with phenol/chloroform, the aqueous layer was transferred to a new centrifuge tube. The DNA was precipitated with ethanol, resuspended in water (100 μL), and treated with RNase A (400 μg/mL) for 2 hr at 37°. Electrophoresis was performed in 1% agarose gel in Tris-borate buffer at about 2V/cm for approximately 14 hr. After electrophoresis, the gel was stained with ethidium bromide (1 mg/mL), washed, and photographed under UV light.

2.11. Apoptosis detection system in fluorescence microscopy

The TUNEL assay developed by Promega was used to identify drug-induced apoptotic HL-60 cells. The supplier's recommended protocol was followed. Briefly, cells were incubated with fluorescein-12-dUTP in the presence of terminal deoxynucleotidyl transferase (TdT) to label 3′-OH ends of fragmented DNA [24]. All cells were stained with propidium iodide. Samples were photographed using a Zeiss Axiophot 2 microscope. Images were captured using the Quick Smart Capture™ software (Vysis).

3. Results

3.1. Cytotoxicity

The cytotoxicity of NB-506 and CPT were evaluated using a conventional tetrazolium-based colorimetric cell proliferation assay. After 48-hr incubation at 37°, the concentrations of NB-506 and CPT required to kill 50% of the cells were 0.78 and 0.40 μM, respectively (IC_{50}). CPT was only slightly more cytotoxic than the indolocarbazole drug with this cell line. For this reason, the drugs were used at identical concentrations for the subsequent experiments designed to determine the mechanism by which NB-506 kills these leukemia cells.

3.2. Cell cycle analysis

The cell cycle distribution of HL-60 cells was analyzed following exposure for 2, 4, and 6 hr to 10 μM drug (Fig. 2). In the control cells, the G1, S, and G2+M populations represented 34, 42, and 21% of the cells, respectively, and the percentages did not vary significantly with time. With NB-506, the cell cycle profile remained unaltered during the first two hours of drug treatment, but changed considerably with the appearance of cells with a DNA content less than G1, which are usually considered as apoptotic cells. The gross alteration in DNA content resulted from degradation of cellular DNA by activation of endogenous nucleases during apoptosis. Approximately 85% and 66% of the cells had a DNA content less than G1 after 4 hr of treatment with CPT and NB-506, respectively. With NB-506, the accumulation of these cells appeared to plateau at about 4–6 hr, with little increase up to 12 hr (not shown). The apoptotic evolution was quicker with CPT: about 40% of sub-G1 cells were already detected after 2 hr of incubation with the drug, and this population was largely predominant after 4 hr. The cell cycle analysis suggests that myeloid leukemia HL-60 cells accomplish apoptosis under NB-506 treatment.

3.3. Mitochondrial membrane potential

The reduction in mitochondrial membrane potential ($\Delta\Psi$mt) accompanying early apoptosis in many experimental systems is believed to be mediated by the opening of the mitochondrial permeability transition pore [25,26]. To investigate whether NB-506 could affect mitochondrial permeability, $\Delta\Psi$mt was monitored by fluorescence of the

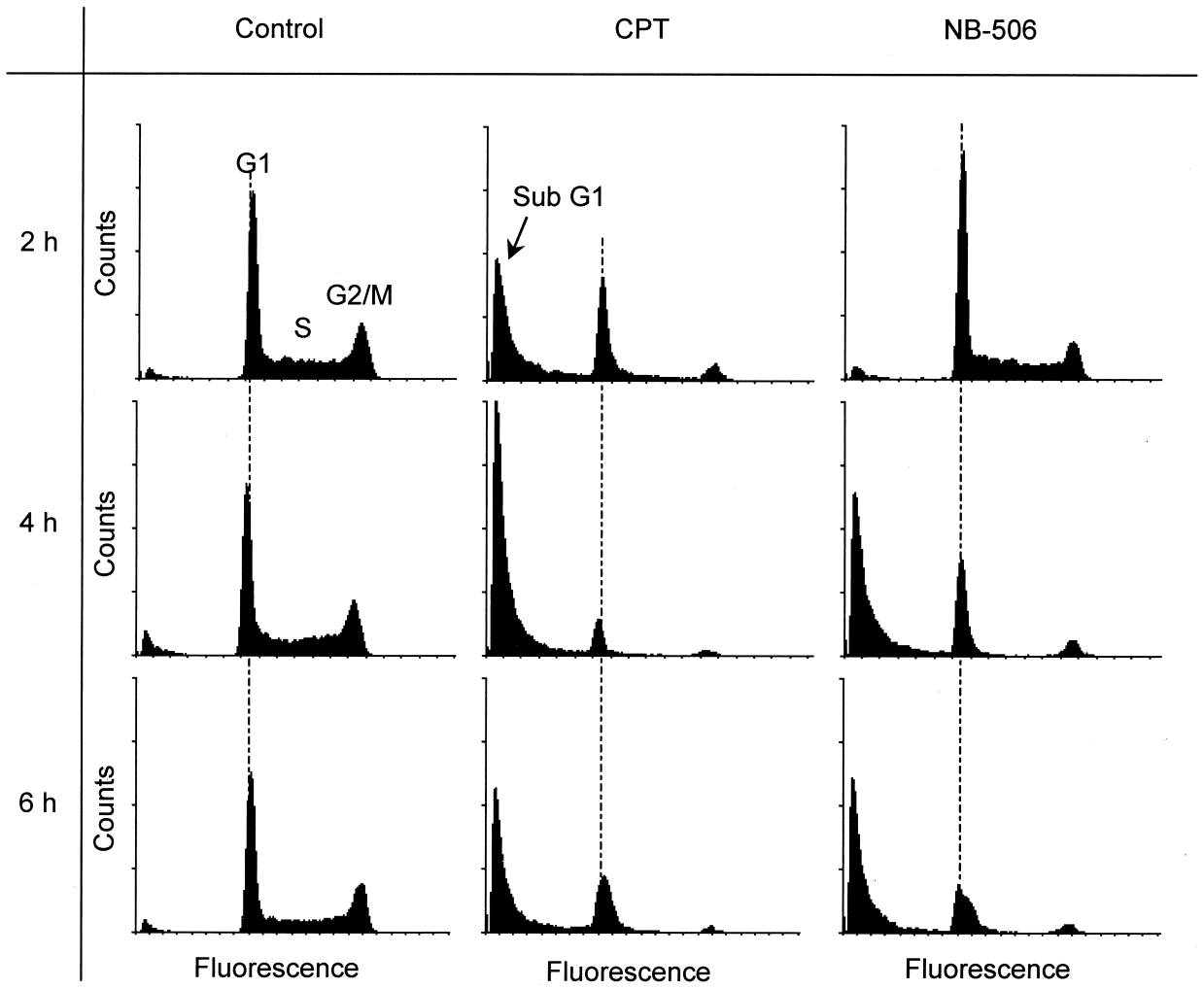

Fig. 2. Cell cycle analysis of both untreated and HL-60 cells treated with 10 μM CPT or NB-506 for 2, 4 and 6 hr. Cells were analyzed with the FACScan flow cytometer as described in Materials and Methods.

cationic lipophilic dye $DiOC_6$. HL-60 cells were treated with 10 μM NB-506 or CPT for 4 hr prior to labeling with 100 nM $DiOC_6$. A marked reduction in fluorescence intensity was observed with both NB-506 and CPT (Fig. 3). A similar decrease in $DiOC_6$ fluorescence was measured using the mitochondrial uncoupling agent carbonyl cyanide *m*-chlorophenylhydrazone (mCICCP), whereas addition of the mitochondrial ATP synthetase inhibitor oligomycin induced a marked increase in fluorescence (not shown). The dissipation of $\Delta\Psi$mt reflects the opening of the mitochondrial permeability transition pores. This effect, which has been commonly observed with other anticancer drugs irrespective of the cell type, generally defines an early but already irreversible stage of apoptosis [27].

3.4. Intracellular pH

A fluorescent method was adopted to measure intracellular pH in cells treated with NB-506 using the dye BCECF. HL-60 cells were loaded with the acetomethyl ester derivative of BCECF (BCECF-AM), a dye whose fluorescence emission is sensitive to pH variations. Cell samples were excited at two wavelengths, 440 and 490 nm, and the emission was recorded at a single wavelength, 535 nm. Ratioing of fluorescence excitation was used as a quantitative measure of the pH, independent of cell volume or dye concentration. The pH of untreated HL-60 cells was 7.44 $\pm$ 0.03. A significant decrease in the pH was observed upon treatment of the cells with CPT or NB-506. In cells treated for 4 hr with drug concentrations ranging from 0.1 to 10 μM, the intracellular pH dropped from 7.4 to 7.1 (Fig. 4). These experiments show that HL-60 cells treated with NB-506 or CPT became significantly more acidic than untreated cells. The extent of the acidic shift depended on the drug concentration but also on the incubation period (data not shown).

3.5. Intracellular calcium

Confirming different studies [28], we found that over the time–course of culture in calcium-containing media, drug-

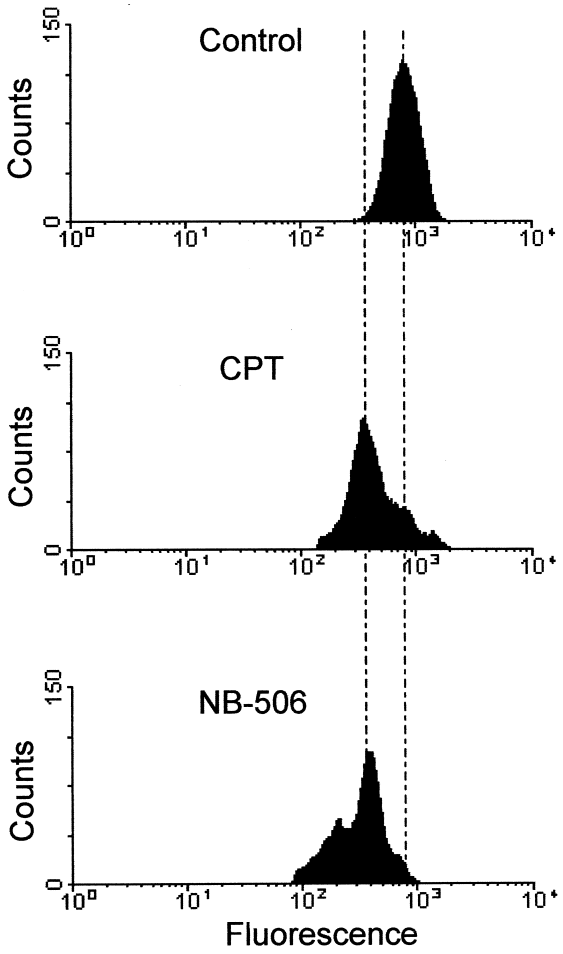

Fig. 3. Depolarization of mitochondrial membranes as a consequence of the drug treatment. The cytofluorometric profiles show the decrease in the fluorescence of the ΔΨmt-sensitive dye $DiOC_6$ upon treatment of HL-60 cells with 10 μM CPT or NB-506 for 4 hr. Cells were stained with 100 nM $DiOC_6$ prior to analysis by flow cytometry.

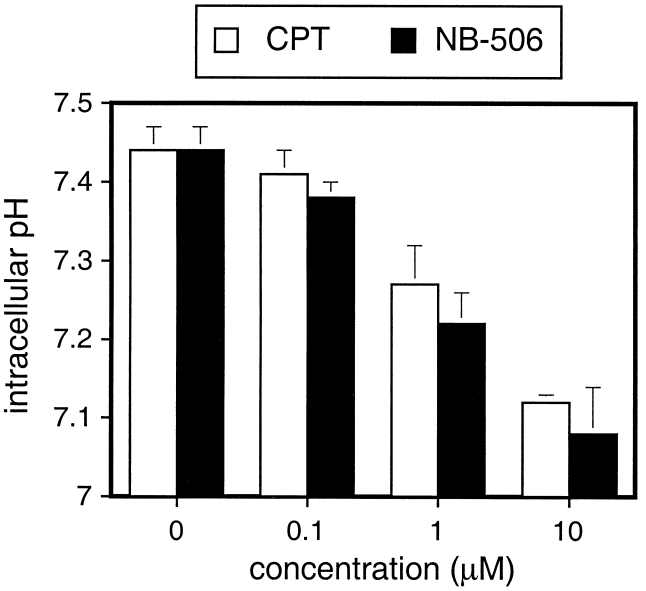

Fig. 4. Changes in intracellular pH induced by NB-506 and CPT in HL-60 cells. Cells were incubated with the test drug at the indicated concentration for 6 hr prior to the fluorescence analysis. Cells were loaded with BCECF-AM and the fluorescence excitation at 440 and 490 nm was measured with an emission at 535 nm. The pH values derive from the average fluorescence ratio for the whole cell population.

treated HL-60 cells undergoing apoptosis demonstrated no elevation of intracellular calcium as measured by the intracellular calcium indicator Fura-2. Control HL-60 cells maintained intracellular Ca^{2+} at 210 ± 9 nM, and no significant changes were seen following treatment of the cells with either CTP, etoposide, or NB-506 (10 μM each for 6 hr). However, the absence of a discernible elevation of intracellular calcium does not exclude the possibility that calcium flux may be required to trigger apoptosis. In fact, Bratton *et al.* [29] have shown that calcium flux is absolutely necessary for the appearance of phosphatidylserines on the outer leaflet of the plasma membrane of HL-60 cells during apoptosis.

3.6. Caspase-3 activation

Studies with genotoxic agents including topoisomerase I inhibitors have shown that programmed cell death is associated with the activation of a number of aspartate-specific cysteine proteases (caspases) [30,31]. In particular, caspase-3 (CPP32, EC 2.4.2.30) is considered essential for the propagation of the apoptotic signal by several types of antitumor drugs [17]. For example, caspase-3, which cleaves DEVD-type substrates, is involved in camptothecin-induced apoptosis in HL-60 cells [32]. It was therefore of interest to determine whether this cysteine protease is also involved in apoptosis induction by NB-506 in HL-60 cells. A first way to address this question is through the use of the caspase-3 peptide substrate DEVD-pNA. We prepared lysates from cells treated for 4 hr with various concentrations of the drug and then assayed for an activity capable of cleaving DEVD-pNA using a solution assay. Lysates were mixed with the pNA-tagged tetrapeptide and the absorbance of the released substrate was recorded at 405 nm using a 96-well plate reader. A marked activity was recorded in lysates from cells treated with 5 and 10 μM NB-506, but the effect was well inferior to that obtained with CPT. NB-506 had no effect at 1 μM, whereas this concentration was sufficient to detect a full activity with CPT. The effect of CPT was comparable to that obtained with drugs such as staurosporine (a protein kinase C inhibitor) and etoposide (a topoisomerase II inhibitor) used as internal positive controls. No activity was detected in the control (drug-free) lysates, and the caspase-3-mediated cleavage activity stimulated by CPT and NB-506 was totally inhibited by the well-characterized inhibitor z-DEVD-fmk (Fig. 5). These results suggest that NB-506 activates caspase-3 with a lower efficiency compared to CPT. However, DEVD is mainly cleaved by caspase-3, but may also be a substrate for caspases-1, -4, -6, -7, and -8 [33]. A recent study of inhibitor

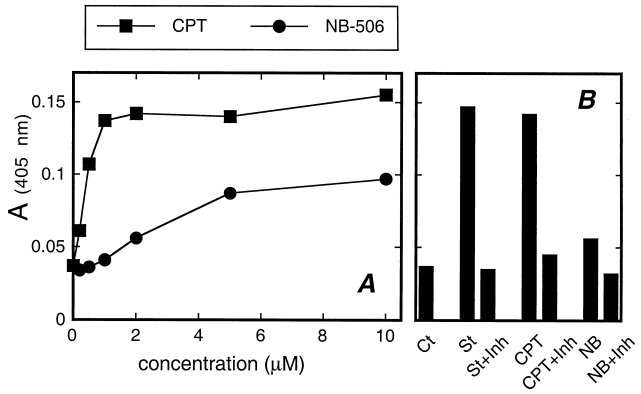

Fig. 5. (a) NB-506 and CPT promote DEVD-pNA cleaving activity. HL-60 cells were incubated with the test drug at the indicated concentration for 4 hr prior to the addition of the caspase-3 substrate DEVD-pNA (50 μM). Assay mixtures were incubated for 1 hr at 37° prior to measurement of absorbance at 405 nm. The histogram in (b) shows the DEVDase activity without drug (control, Ct) and in the presence of 0.1 μM staurosporine (St), 2 μM NB-506 (NB), 2 μM camptothecin (CPT), with or without the peptidic inhibitor of caspase-3 DEVD-fmk at 5 μM (+Inh). Results are the means of three experiments.

specificity found that z-DEVD-fmk inhibits both caspases-3 and -7 [34,35]. Therefore, we used a second method to probe the involvement of caspase-3 in NB-506-induced apoptosis.

Poly(ADP-ribose) polymerase (PARP), an enzyme involved in DNA repair, is a preferential substrate for caspase-3 [36]. We determined the extent of PARP cleavage by immunoblot analysis and densitometric analysis of the PARP cleavage product. The time–courses of CPT- and NB-506-induced cleavage of PARP were compared. Fig. 6

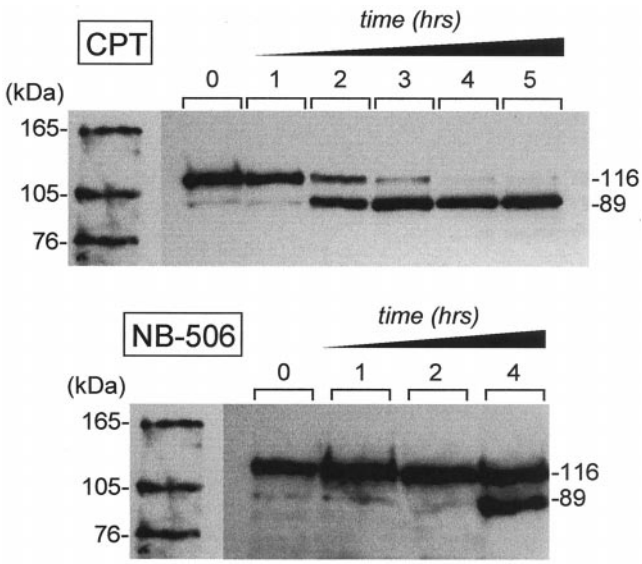

Fig. 6. Induction of PARP cleavage by CPT and NB-506. Western blot was used to detect the cleavage of full-length PARP [116-kDa band] into the 89-kDa fragment in untreated cells (Ct) and cells treated with CPT or NB-506 (10 μM each) for 1–5 hr. Whole cell lysates were subjected to SDS–PAGE followed by blotting with an anti-PARP monoclonal antibody.

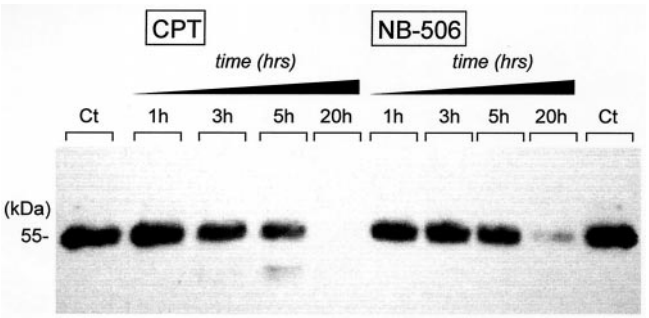

Fig. 7. Activation of caspase-8 by CPT and NB-506. Western blot was used to detect cleavage of caspase-8 [55-kDa band] in untreated cells (Ct) and cells treated with CPT or NB-506 (10 μM each) for 1–20 hr. Whole cell lysates were subjected to SDS–PAGE followed by blotting with an anti-caspase-8 monoclonal antibody.

shows PARP cleavage in control cells and cells treated with 10 μM topoisomerase I inhibitor for up to 5 hr as examined by Western blot. CPT was very efficient at inducing PARP cleavage, as reflected by the intensity of the 89,000 MW PARP fragment. Quantitative cleavage was observed after 4 hr of treatment with CPT. NB-506 also induced caspase-3-mediated PARP cleavage, but with a much lower efficiency. Only about 50% of endogenous PARP was cleaved after 5 hr of treatment of HL-60 cells with NB-506. Cleavage reached approximately 70% after 6 hr, and quantitative cleavage required at least 12 hr of drug treatment (data not shown).

3.7. Caspase-8 activation

Caspase-3 is an executioner protease that can be activated by at least two distinct mechanisms. Cytochrome *c*, which is often released from the mitochondria into the cytosol [37], can induce ATP- or dATP-dependent formation of a complex of proteins that results in the proteolytic activation of pro-caspase-3 and the apoptotic destruction of the nuclei [38]. Alternatively, distal caspases such as caspases-3, -6, and -7 can be directly activated by a proximal caspase such as caspase-8 [39,40]. The caspase-8 and cytochrome *c* pathways for caspase-3 activation are both independent, and inhibited by IAP (inhibitor of apoptosis) proteins at distinct points [41]. However, caspase-8 can also act through mitochondria to facilitate the efflux of cytochrome *c* [42]. These considerations prompted us to examine the variation in the intracellular levels of caspase-8 in HL-60 cells treated with NB-506.

HL-60 cells were treated with 10 μM NB-506 or CPT for 1, 3, 5, or 20 hr, and the processing of caspase-8 was detected by immunoblot analysis (Fig. 7). Caspase-8 was synthesized as two isoforms of ~55 kDa which comigrated into a single product under our electrophoretic conditions. Band intensities of different blots were quantified by densitometry. After 3 hr of incubation with the drugs, the intensity of the caspase-8 product was decreased by 32 and

23% with CPT and NB-506, respectively. The band was decreased by about 50% after 5-hr treatment of the cells with CPT, whereas the same band was decreased by only 25% with NB-506. The processing of caspase-8 was considerably higher when the cells were incubated overnight with the drugs. These experiments indicate that both topoisomerase I inhibitors activate caspase-8 and that the extent of activation is more pronounced with CPT than with NB-506. Similar results were obtained using a colorimetric assay.

To further investigate the activation of caspase-8, we measured the rate of IETD-pNA hydrolysis in cells treated with graded concentrations of NB-506 or CPT for 4 or 18 hr (Fig. 8). A marked IETDase activity was recorded in lysates from cells treated with NB-506 or CPT, but here again the effect was weaker with the indolocarbazole drug compared to CPT after 4 hr of treatment (Fig. 8A). In contrast, there was no significant difference between the two drugs when the drug treatment period was extended to 18 hr (Fig. 8C). As for caspase-3, we found that the peptidase-induced activity of NB-506 and CPT (as well as staurosporine used as a control) was abolished upon addition of the inhibitory peptide z-Ile-Glu-Thr-Asp-fluoromethylketone (z-IETD-fmk) (Fig. 8B). Together with the Western blot experiments presented in Fig. 7, these results clearly indicate that NB-506 activates caspase-8.

3.8. DNA fragmentation

To assess the extent of DNA digestion following short exposure to the topoisomerase I poisons, HL-60 cells were treated for 2 hr with 10 μM NB-506 or CPT. Untreated control cells contained only high-molecular-weight DNA. In contrast, both NB-506 and CPT caused the production of lower-molecular-weight DNA fragments consisting of multimers of 180 base pairs (Fig. 9). The cleavage patterns are typical of internucleosomal DNA digestion by an endogenous nuclease considered characteristic of apoptotic cell death [43].

Another detection system, the TUNEL assay, was also employed to characterize drug-induced genomic DNA cleavage. Unlike detection by the above-mentioned "DNA ladder" on agarose gels, the TUNEL method detects apoptosis at a single-cell level and thus permits a better evaluation of the apoptotic cell fraction [24]. The technique is based on the fluorescein labeling of apoptotic DNA fragments. Fig. 10 shows immunofluorescent pictures of HL-60 cells treated with NB-506 or CPT. Control cells containing intact genomic DNA appeared in red (due to staining with propidium iodide), whereas a considerable number of apoptotic cells colored in green were detected by fluorescence microscopy within the population of cells treated with 10 μM NB-506 for 6 hr (Fig. 10). We counted the number of apoptotic cells in several fields. Approximately 60% of the cells were positive (green cells divided by the number of red cells per field). The apoptosis rate in the control cells was less than 2%. A similar 30-fold increase in the apoptosis rate was measured in suspension cells using flow cytometry (data not shown). Brightly fluorescent green cells were also detected with CPT. In this case, almost all cells were positive. The DNA laddering and TUNEL assays concur that NB-506 induces DNA digestion in HL-60 cells.

4. Discussion

The results clearly indicate that the antitumor drug NB-506 targeting topoisomerase I induces apoptosis in chemosensitive HL-60 cells. Upon treatment of the cells with NB-506 or CPT, caspase-8 is cleaved, leading to a downstream caspase cascade activation involving caspase-3. Caspase-8 is proximal to the Fas ligand (Fas-L) receptor. Induction of Fas-L and up-regulation of Fas after treatment with cytotoxic drugs such as doxorubicin have been observed in a variety of tumor cells [44,45]. However, in our case, we could not detect Fas in HL-60 cells treated with NB-506 by Western blot using a monoclonal antibody raised against Fas (Pharmingen) (data not shown). Other groups have reported that there is no activation of Fas in HL-60 cells upon treatment with cytotoxic drugs, including topoisomerase inhibitors [46,47]. It is now widely accepted that drug-triggered apoptosis can occur independently of the Fas/Fas-L system, apparently by directly perturbing mitochondrial functions [48,49]. In the same vein, our results indicate that apoptosis induced by drugs like CPT and NB-506 does not require changes in the intracellular calcium level, at least in the HL-60 cell line. HL-60 cells stably express the apoptosis-suppressive gene *bcl-2* [50], but are p53-null [51,52].

Alterations of the mitochondrial functions play a major role in the apoptotic process, in particular in cell death induced by chemotherapeutic agents [26]. It is highly likely that NB-506 provokes marked changes in these mitochondrial functions, as judged from both the loss of the mitochondrial membrane potential ($\Delta\Psi$mt) and the significant drop in intracellular pH in drug-treated cells versus control cells. The collapse of $\Delta\Psi$mt is a signature of the opening of the mitochondrial pores responsible for an uncoupling of the respiratory chain and efflux of small molecules (e.g. cytochrome *c*, calcium) and certain proteins including caspases-2 and -9 [53] as well as the apoptosis-inducing factor (AIF), which can in turn stimulate the proteolytic activation of caspase-3 [54]. However, caspases can act either upstream or downstream of mitochondria [26,37]. For example, caspase-8 activation occurs downstream of the $\Delta\Psi$mt dissipation in apoptosis induced by betulinic acid, whereas caspase-8 cleavage occurs upstream of the $\Delta\Psi$mt collapse in doxorubicin-induced apoptosis [55]. The drug-induced opening of the permeability transition pores also causes the release of protons into the cytosol, contributing to the intracellular acidification process that we monitored by fluorescence using the BCECF probe. Lowering the pH can

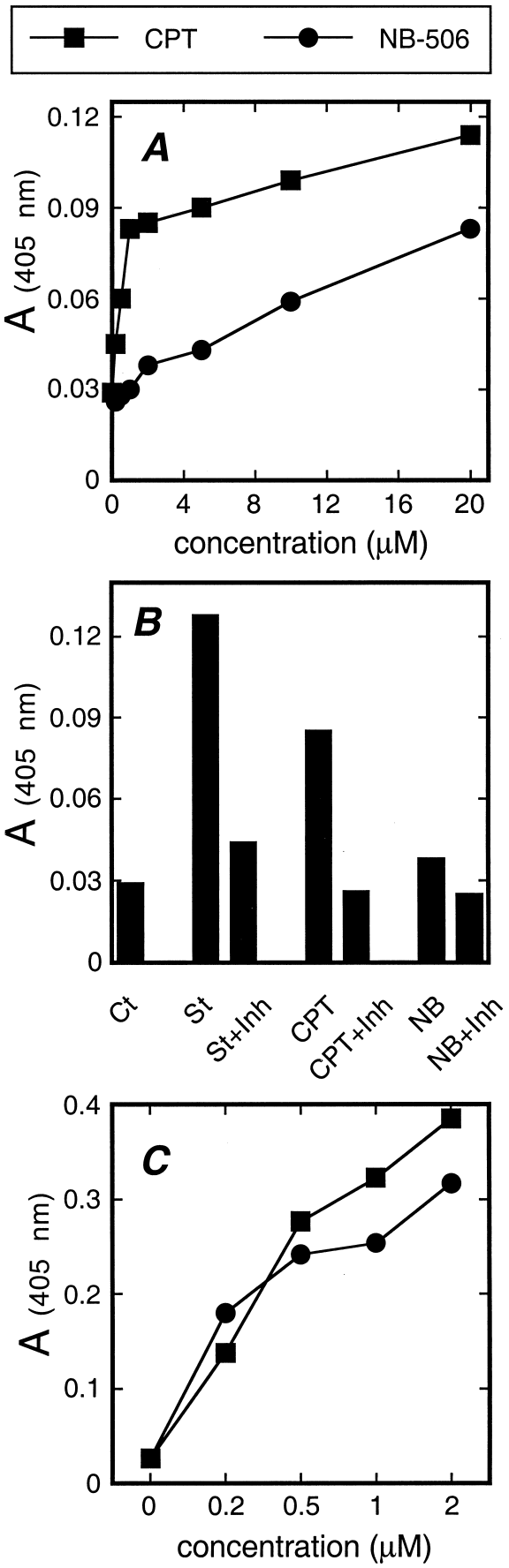

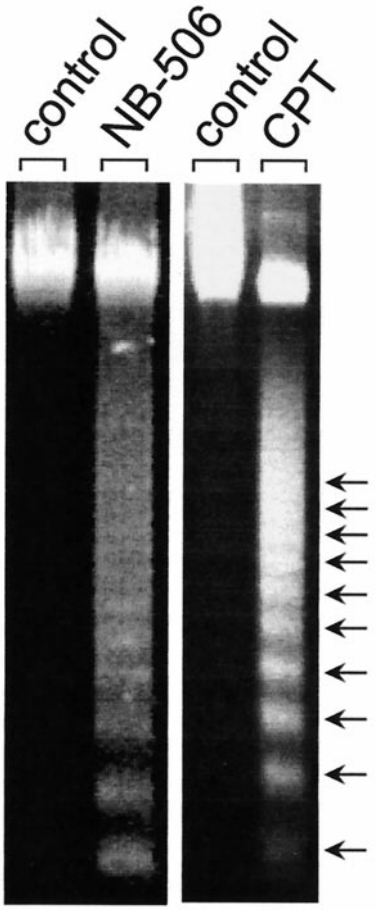

Fig. 9. Agarose gel electrophoresis of DNA extracted from untreated HL-60 cells (control) and cells treated with 10 μM NB-506 or CPT for 4 hr. DNA was stained with ethidium bromide after electrophoresis on a 1% agarose gel and then visualized under UV light. Oligonucleosome-sized DNA fragmentation can be clearly seen in drug-treated cells (arrows).

induce apoptosis by itself in HL-60 cells [56]. Intracellular acidification is often considered a consequence of the mitochondrial proton leak, but may be also a cause rather than a consequence of the loss of $\Delta\Psi$mt [57]. A drug-induced increase in the proton permeability of the mitochondrial inner membrane can lead to a decrease in mitochondrial membrane potential [58]. Therefore, the pH changes may serve to modulate the apoptotic responsiveness of the cell, as well as amplifying the apoptotic program.

The way in which NB-506 activates the apoptotic ma-

Fig. 8. NB-506 and CPT promote IETD-pNA cleaving activity. HL-60 cells were incubated with the test drug at the indicated concentration for (a) 4 hr or (c) 18 hr prior to the addition of the caspase-8 substrate IETD-pNA (50 μM). Assay mixtures were incubated for 1 hr at 37° prior to measurement of absorbance at 405 nm. The histogram in (b) shows the IETDase activity without drug (control, Ct) and in the presence of 0.1 μM staurosporine (St), 2 μM NB-506 (NB), 2 μM camptothecin (CPT), with or without the peptidic inhibitor of caspase-3 DEVD-fmk at 5 μM (+Inh) for 4 hr. Results are the means of three experiments.

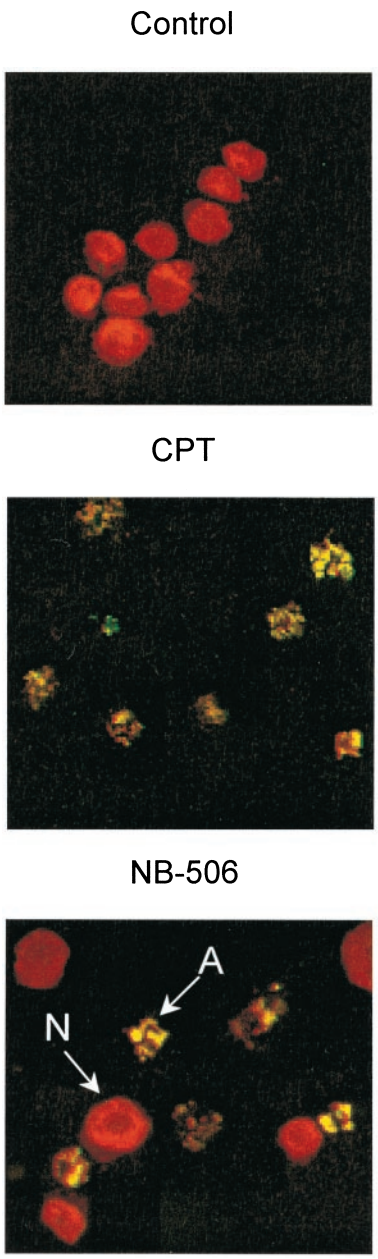

Fig. 10. Characterization of drug-induced DNA cleavage in HL-60 cells with the TUNEL assay. (N) Non-apoptotic cells with intact genomic DNA appear in red, whereas fragmented DNA in cells undergoing apoptosis (A) is labeled with fluorescein, providing green cells. Cells were treated with 10 μM CPT or NB-506 for 6 hr prior to the fluorescein labeling. Control refers to the untreated cells.

chinery appears very similar to CPT-induced activation. Both the indolocarbazole derivative and camptothecin provoke a collapse of $\Delta\Psi$mt, reduce intracellular pH, stimulate caspases-3 and -8, and cause DNA fragmentation into oligonucleosomes. Although the two drugs are almost equally toxic to HL-60 cells, the apoptotic effects are generally less pronounced with NB-506 than with CPT. The results in Figs. 5–8 clearly show that NB-506 is less efficient than CPT at activating caspases-3 and -8. After 4 hr of treatment with NB-506, only about 50% of PARP is cleaved in HL-60 cells, whereas the same treatment with CPT produces quantitative cleavage of the polymerase. Therefore, it seems difficult to establish a relationship between drug cytotoxicity and the magnitude of the apoptotic response in HL-60 cells. Different rates of penetration of the two drugs in HL-60 cells may account for the reduced or delayed apoptotic effects observed with NB-506 compared to CPT. We have recently shown that the uptake of a glycosylated indolocarbazole derivative of NB-506 in HL-60 cells is rapid but limited to about 6% of the drug molecules [59].

In conclusion, the study reported here provides for the first time direct evidence that the promising antitumor drug NB-506 induces apoptosis in leukemia cells. There is no doubt that mitochondria and caspases play a central role in the activation of the executioner phase of NB-506-induced apoptosis. Inhibition of topoisomerase I likely serves as the inducing signal triggering mitochondrial activation. However, further investigations are warranted to identify the signal(s), downstream of topoisomerase I and upstream of mitochondria, involved in activation of the apoptosis machinery. Identifications of these specific targets may have profound therapeutic implications.

Acknowledgment

The authors thank Nicole Wattez and Christine Mahieu for expert technical assistance and Dr. A. Lansiaux for useful advice. The protocol for the caspase-8 experiments was provided by Olivier Sordet (Inserm U-517, Dijon, France). We thank also the *Service Commun d'Imagerie Cellulaire de l'IFR22* for access to the fluorescence microscope. This work was supported by research grants (to C.B.) from the Association pour la Recherche sur le Cancer.

References

[1] Arakawa H, Iguchi T, Morita M, Yoshinari T, Kojiri K, Suda H, Okura A, Nishimura S. Novel indolocarbazole compound 6-*N*-formylamino-12,13-dihydro-1,11-dihydroxy-13-(β-D-glucopyranosyl)-5*H*-indolo[2,3-*a*]pyrrolo-[3,4-*c*]carbazole-5,7-(6*H*)-dione (NB-506): its potent antitumor activities in mice. Cancer Res 1995;55:1316–20.

[2] Yoshinari T, Matsumoto M, Arakawa H, Okada H, Noguchi K, Suda H, Okura A, Nishimura S. Novel antitumor indolocarbazole compound 6-*N*-formylamino-12,13-dihydro-1,11-dihydroxy-13-(β-D-glucopyranosyl)-5*H*-indolo[2,3-*a*]pyrrolo-[3,4-*c*]carbazole-5,7-(6*H*)-dione (NB-506): induction of topoisomerase I-mediated DNA cleavage and mechanisms of cell line-selective cytotoxicity. Cancer Res 1995;55:1310–15.

[3] Ohe Y, Tanigawara Y, Fujii H, Ohtsu T, Wakita H, Igarashi T, Minami H, Eguchi K, Shinkai T, Tamura T, Kunotoh H, Saijo N, Okada K, Ogino H, Sasaki Y. Phase I and pharmacology study of 5-day infusion of NB-506. Proc ACSO 1997;16:199a.

[4] Saijo N. New chemotherapeutic agents for the treatment of non-small cell lung cancer. Chest 1998;(Suppl 1):113:17S–23S.

[5] Yamashita Y, Fujii N, Murakata C, Ashizawa T, Okabe M, Nakano H. Induction of mammalian DNA topoisomerase I mediated DNA

cleavage by antitumor indolocarbazole derivatives. Biochemistry 1992;31:12069–75.
[6] Yoshinari T, Yamada A, Uemura D, Nomura K, Arakawa H, Kojiri K, Yoshida E, Suda H, Okura A. Induction of topoisomerase I-mediated DNA cleavage by a new indolocarbazole, ED-110. Cancer Res 1993;53:490–4.
[7] Bailly C, Riou JF, Colson P, Houssier C, Rodrigues-Pereira E, Prudhomme M. DNA cleavage by topoisomerase I in the presence of indolocarbazole derivatives of rebeccamycin. Biochemistry 1997;36:3917–29.
[8] Bailly C, Qu X, Chaires JB, Colson P, Houssier C, Ohkubo M, Nishimura S, Yoshinari T. Substitution at the F-ring N-imide of the indolocarbazole antitumor drug NB-506 increases the cytotoxicity, DNA binding and topoisomerase I inhibition activities. J Med Chem 1999;42:2927–35.
[9] Bailly C, Dassonneville L, Colson P, Houssier C, Fukasawa K, Nishimura S, Yoshinari T. Intercalation into DNA is not required for inhibition of topoisomerase I by indolocarbazole antitumor agents. Cancer Res 1999;59:2853–60.
[10] Bailly C, Colson P, Houssier C, Rodrigues-Pereira E, Prudhomme M, Waring MJ. Recognition of specific sequences in DNA by a topoisomerase I inhibitor derived from the antitumor drug rebeccamycin. Mol Pharmacol 1998;53:77–87.
[11] Bailly C, Qu X, Graves DE, Prudhomme M, Chaires JB. Calories from carbohydrates: energetic contribution of the carbohydrate moiety of rebeccamycin to DNA binding and the effect of its orientation on topoisomerase I inhibition. Chem Biol 1999;6:277–86.
[12] Bailly C, Carrasco C, Hamy F, Vezin H, Prudhomme M, Saleem A, Rubin E. The camptothecin-resistant topoisomerase I mutant F361S is cross-resistant to antitumor rebeccamycin derivatives. A model for topoisomerase I inhibition by indolocarbazoles. Biochemistry 1999;38:8605–11.
[13] Kanzawa F, Nishio K, Kubota N, Saijo N. Antitumor activities of a new indolocarbazole substance, NB-506, and establishment of NB-506-resistant cell lines, SBC-3/NB. Cancer Res 1995;55:2806–13.
[14] Komatani H, Morita M, Sakaizumi N, Fukasawa K, Yoshida E, Okura A, Yoshinari T, Nishimura S. A new mechanism of acquisition of drug resistance by partial duplication of topoisomerase I. Cancer Res 1999;59:2701–8.
[15] Labourier E, Riou JF, Prudhomme M, Carrasco C, Bailly C, Tazi J. Poisoning of topoisomerase I by an antitumor indolocarbazole drug: stabilization of topoisomerase I–DNA covalent complexes and specific inhibition of the protein kinase activity. Cancer Res 1999;59:52–55.
[16] Solary E, Bertrand R, Pommier Y. Apoptosis induced by DNA topoisomerase I and II inhibitors in human leukemic HL-60 cells. Leuk Lymphoma 1994;15:21–32.
[17] Kaufman SH. Cell death induced by topoisomerase-targeted drugs: more questions than answers. Biochim Biophys Acta 1998;1400:195–211.
[18] Ohkubo M, Kawamoto H, Ohno T, Nakano M, Morishima H. Synthesis of NB-506, a new anticancer agent. Tetrahedron 1997;53:585–92.
[19] Cory AH, Owen TC, Barltrop JA, Cory JG. Use of an aqueous soluble tetrazolium/formazan assay for cell growth assays. Cancer Commun 1991;3:207–12.
[20] Negulescu PA, Machen TE. Intracellular ion activities and membrane transport in parietal cells measured with fluorescent dyes. Methods Enzymol 1990;192:38–81.
[21] Goossens JF, Hénichart JP, Dassonneville L, Facompré M, Bailly C. Relation between intracellular acidification and camptothecin-induced apoptosis in leukemia cells. Eur J Pharm Sci 2000;10:125–31.
[22] Grynkiewicz G, Poenie M, Tsien RY. A new generation of Ca^{2+} indicators with greatly improved fluorescence properties. J Biol Chem 1985;260:3440–50.
[23] Kao JP. Practical aspects of measuring $[Ca^{++}]$ with fluorescent indicators. Methods Cell Biol 1994;40:155–81.
[24] Ben-Sasson SA, Sherman Y, Gavrieli Y. Identification of dying cells—*in situ* staining. Methods Cell Biol 1995;46:29–39.
[25] Zarotti M, Szabo I. The mitochondrial permeability transition. Biochim Biophys Acta 1995;1241:139–79.
[26] Kroemer G, Zamzami N, Susin SA. Mitochondrial control of apoptosis. Immunol Today 1997;18:44–51.
[27] Kroemer G, Dallaporta B, Resche-Rigon M. The mitochondrial death/life regulator in apoptosis and necrosis. Annu Rev Physiol 1998;60:619–42.
[28] Lennon SV, Kifeather SA, Hallett MB, Campbell AK, Cotter TG. Elevations in cytosolic free Ca^{2+} are not required to trigger apoptosis in human leukemia cells. Clin Exp Immunol 1992;87:465–71.
[29] Bratton DL, Fadok VA, Richter DA, Kailey JM, Guthrie LA, Henson PM. Appearance of phosphatidylserine on apoptotic cells requires calcium-mediated nonspecific flip-flop and is enhanced by loss of the aminophospholipid translocase. J Biol Chem 1999;272:26159–65.
[30] Kidd V. Proteolytic activities that mediate apoptosis. Annu Rev Physiol 1998;60:533–73.
[31] Nuñez G, Benedict M, Hu Y, Inohara N. Caspases: the proteases of the apoptotic pathway. Oncogene 1998;17:3237–45.
[32] Shimizu T, Pommier Y. Camptothecin-induced apoptosis in p53-null human leukemia HL60 cells and their isolated nuclei: effects of the protease inhibitors Z-VAD-fmk and dichloroisocoumarin suggest an involvement of both caspases and serine proteases. Leukemia 1997;11:1238–44.
[33] Talanian RV, Quinlan C, Trautz S, Hackett MC, Mankovich JA, Banach D, Ghayur T, Brady KD, Wong WW. Substrate specificity of caspase family proteases. J Biol Chem 1997;272:9677–82.
[34] Villa P, Kaufmann SH, Earnshaw WC. Caspases and caspase inhibitors. Trends Biochem Sci 1997;22:388–93.
[35] Garcia-Calvo M, Peterson EP, Rasper DM, Vaillancourt JP, Zamboni R, Nicholson DW, Thornberry NA. Purification and catalytic properties of human caspase family members. Cell Death Differ 1999;6:362–9.
[36] Tewari M, Quan LT, O'Rourke K, Desnoyers S, Zeng Z, Beidler DR, Poirier GG, Salvesen GS, Dixit VM. Yama/CPP32 beta, a mammalian homolog of CED-3, is a CrmA-inhibitable protease that cleaves the death substrate poly(ADP-ribose) polymerase. Cell 1995;81:801–9.
[37] Bossy-Wetzel E, Newmeyer DD, Green DR. Mitochondrial cytochrome *c* release in apoptosis occurs upstream of DEVD-specific caspase activation and independently of mitochondrial transmembrane depolarization. EMBO J 1998;17:37–49.
[38] Liu X, Kim CN, Yang J, Jemmerson R, Wang X. Induction of apoptotic program in cell-free extracts: requirement for dATP and cytochrome *c*. Cell 1996;86:147–57.
[39] Muzio M, Salvesen GS, Dixit VM. FLICE induced apoptosis in a cell-free system. Cleavage of caspase zymogens. J Biol Chem 1997;272:2952–6.
[40] Stennicke HR, Jürgensmeier JM, Shin H, Deveraux Q, Wolf BB, Yang X, Zhou Q, Ellerby HM, Ellerby LM, Bredesen D, Green DR, Reed JC, Froelich CJ, Salvesen GS. Pro-caspase-3 is a major physiologic target of caspase-8. J Biol Chem 1998;273:27084–90.
[41] Deveraux QL, Roy N, Stennicke HR, Van Arsdale T, Zhou Q, Srinivasula SM, Alnemri ES, Salvesen GS, Reed JC. IAPs block apoptotic events induced by caspase-8 and cytochrome *c* by direct inhibition of distinct caspases. EMBO J 1998;17:2215–23.
[42] Kuwana T, Smith JJ, Muzio M, Dixit V, Newmeyer DD, Kornbluth S. Apoptosis induction by caspase-8 is amplified through the mitochondrial release of cytochrome *c*. J Biol Chem 1998;273:16589–94.
[43] Compton MM. A biochemical hallmark of apoptosis: internucleosomal degradation of the genome. Cancer Metastasis Rev 1992;11:105–19.
[44] Friesen C, Herr I, Krammer PH, Debatin KM. Involvement of the CD95 (APO-1/Fas) receptor/ligand system in drug-induced apoptosis in leukemia cells. Nat Med 1996;2:574–7.

[45] Russo M, Palumbo R, Tedesco I, Mazzarella G, Russo P, Iacomino G, Russo GL. Quercetin and anti-CD95 (Fas/Apo1) enhance apoptosis in HPB-ALL cell line. FEBS Lett 1999;462:322–8.
[46] Eischen CM, Kottke TJ, Martins LM, Basi GS, Tung JS, Earnshaw WC, Leibson PJ, Kaufmann SH. Comparison of apoptosis in wild-type and Fas-resistant cells: chemotherapy-induced apoptosis is not dependent on Fas/Fas ligand interactions. Blood 1997;90:935–43.
[47] Siitonen T, Mantymaa P, Saily M, Savolainen ER, Koistinen P. Etoposide-induced apoptosis is not associated with the Fas pathway in acute myeloblastic leukemia cells. Leukemia Res 2000;24:281–8.
[48] Fulda S, Friesen C, Los M, Scaffidi C, Mier W, Benedict M, Nuñez G, Krammer PH, Peter ME, Debatin KM, Galle PR. Betulinic acid triggers CD95 (APO-1/Fas)- and p53-independent apoptosis via activation of caspases in neuroectodermal tumors. Cancer Res 1997;57:4956–64.
[49] Watson A. The role of Fas in apoptosis induced by anticancer drugs. Hepatology 1999;29:280–1.
[50] Delia D, Aieuo A, Soligo D, Fontanella E, Melani C, Pezzella F, Pierotti MA, Della Porta G. bcl-2 proto-oncogene expression in normal and neoplastic human myeloid cells. Blood 1992;79:1291–8.
[51] Wolf D, Rotter V. Major deletions in the gene encoding the p53 tumor antigen cause lack of p53 expression in HL-60 cells. Proc Natl Acad Sci USA 1985;82:790–4.
[52] Collins SJ. The HL-60 promyelocytic leukemia cell line: proliferation, differentiation and cellular oncogene expression. Blood 1987;82:15–21.
[53] Susin SA, Lorenzo HK, Zamzami N, Marzo I, Brenner C, Larochette N, Prévost MC, Alzari PM, Kroemer G. Mitochondrial release of caspase-2 and -9 during the apoptotic process. J Exp Med 1999;189:381–93.
[54] Susin SA, Zamzami N, Castedo M, Daugas E, Wang HG, Geley S, Fassy F, Reed JC, Kroemer G. The central executioner of apoptosis: multiple links between protease activation and mitochondria in Fas/Apo-1/CD95- and ceramide-induced apoptosis. J Exp Med 1997;186:25–37.
[55] Fulda S, Susin SA, Kroemer G, Debatin KM. Molecular ordering of apoptosis induced by anticancer drugs in neuroblastoma cells. Cancer Res 1998;58:4453–60.
[56] Park HJ, Makepeace CM, Lyons JC, Song CW. Effect of intracellular acidity and ionomycin on apoptosis in HL-60 cells. Eur J Cancer 1996;32A:540–6.
[57] Shrode LD, Tapper H, Grinstein S. Role of intracellular pH in proliferation, transformation, and apoptosis. J Bioenerg Biomembr 1997;29:393–9.
[58] Steen H, Maring JG, Meijer DK. Differential effect of metabolic inhibitors on cellular and mitochondrial uptake of organic cations in rat liver. Biochem Pharmacol 1993;45:809–18.
[59] Goossens JF, Hénichart JP, Anizon F, Prudhomme M, Dugave C, Riou JF, Bailly C. Cellular uptake and interaction with purified membranes of rebeccamycin derivatives. Eur J Pharmacol 2000;389:141–6.